



Numerical modeling of a fiber optic sensor in its environment for civil engineering applications

M. Barbachi^{*}, F. Bourquin^{}**

^{*}*ENSA, National School of Applied Sciences - BP 1136 Agadir - Morocco,*

^{**}*IFSTTAR-LCPC; 58, boulevard Lefebvre 75732 Paris Cedex 15 – France*

Received 19 June 2012, Revised 30 July 2012, Accepted 30 July 2012

* Corresponding author. E mail: barbachi@ensa-agadir.ac.ma, Tel. : +212 5 28 22 83 13

Abstract

In this paper, we developed a numerical modeling of a sensor composed of a single mode optical fiber inserted between two thin steel ribbons that are embedded in a polyurethane-type material. The different steps of calculation are performed using the method of finite element discretization. From a mechanical view point, the ribbon transfers its applied external loading to the fiber in the unidirectional form. This transmission causes birefringence in the optical fiber by modifying the opto-geometrical parameters related to the difference between principal stresses in the fiber core. The polarization phase shift enables to evaluate the applied load. The application of this study is about the development of an instrumentation dedicated to the analysis of road traffic (vehicle WIM).

The numerical results presented, show the behavior of the sensor as a function of the ribbon geometry for elastic massive under load. These results should be validated from experiments taking into account environmental characteristics and conditions of use.

Keywords: Fiber optic sensors, birefringence, elasto-optical coupling, mechanical modeling, finite elements.

1. Introduction

The primary function of optical fibers is to transmit information over long distances via light waves located in the spectral range extending from visible to near infrared [1]. These are the optical guides, generally with a cylindrical symmetry, consist of a core and optical cladding of silica, all protected by a mechanical cladding. From the eighties, many laboratories have studied seriously the way of measuring certain physical quantities using optical fibers [2], [3], [4] and [5]. However, although there is a rich literature on the principles of sensors and their intrinsic responses, very few studies have approached their response extrinsic, i.e., taking into account the environment of sensor employment [6], [7], [8], [9], [10], [11] and [12]. It is precisely the subject of this work.

2. Sensor inserted in a massive

The sensor consists of a single mode optical fiber inserted between two steel ribbons welded at the edges [13] and [14]. The sensor is then placed on the lower support of a metallic U tube. This tube is filled with a

polyurethane elastic material subjected to uniform load that simulating the rolling load of a vehicle (figure 1). The insertion of the sensor in the elastic medium is motivated by several reasons. First, this arrangement is a good physical and chemical protection of the sensor, and then it allows a better distribution of the load applied to the sensor. From a mechanical point of view, the essential role of ribbon is to integrate the external forces applied to the fiber in a single direction. This transmission induces, by modifying the opto-geometric parameters, a birefringence in the fiber directly related to the difference of principal stresses in the fiber core and whose measurement allows to determine quantitatively inducing actions (i.e. the external forces). In mechanical terms, the problem is to determine the stress state in the fiber core for different geometries of the ribbon when the massive is subjected to a uniformly distributed load.

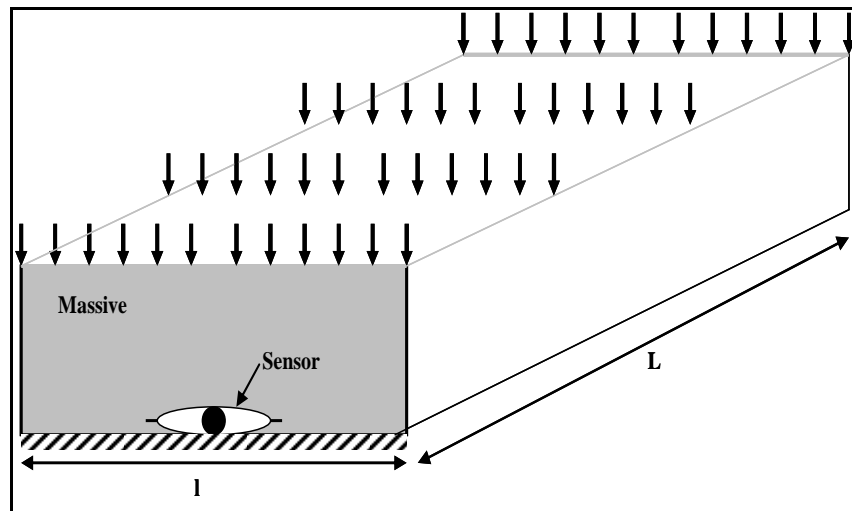


Figure 1: Structure of the sensor inserted into a massive

3. Mechanical modeling

The assumption of plane strain (PS) has been adopted because of the problem dimensions (l / L). In the first approach, to simplify the model studied, we took into account the symmetry of the massive and the sensor, and the uniformity of loading. This is equivalent to treat half of the elastic model with appropriate boundary conditions, figure 2.

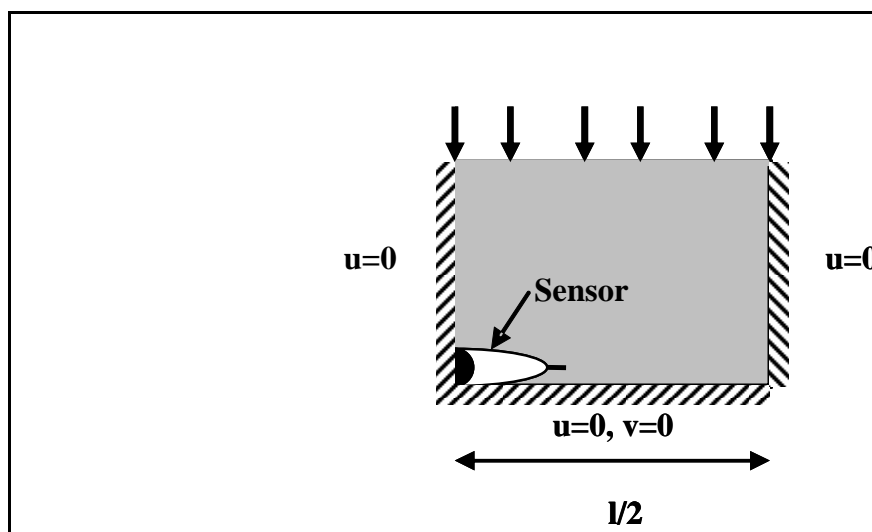


Figure 2: Front view of model

In the second approach, we modeled the ribbon with a straight beam laying on two supports respectively elastic and rigid. In these conditions, the first type of support, characterized by a variable stiffness K , simulates the behavior of the optical fiber; and the second, is modeling the physical link between two ribbons. The final problem is therefore to model the structure described in figure 3.

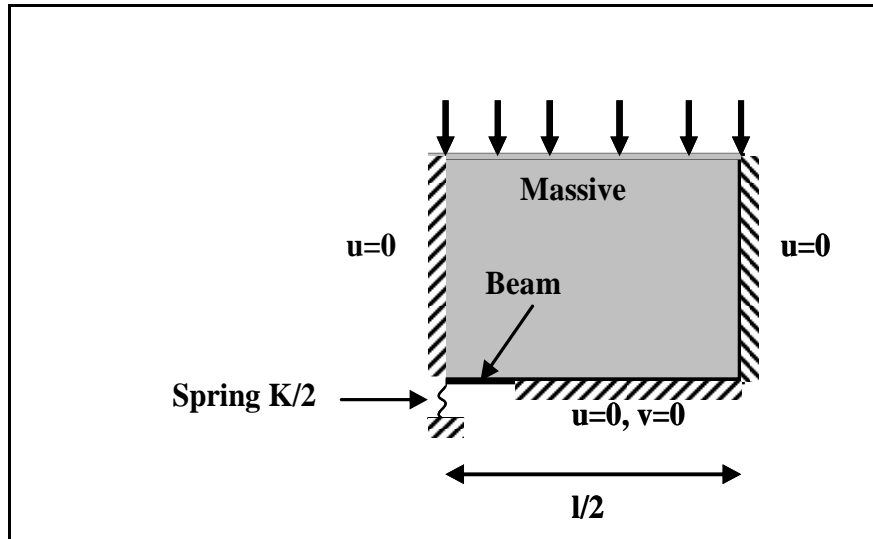


Figure 3: The simplified model

Resolution of the problem is to extract the reaction of the beam at the support modeling elastic fiber when the massive is subjected to uniform loading and this is for different geometries of ribbon. This reaction is then applied to the optical fiber placed between two rigid planes developing a contact surface as a function of the load.

Given the fact that the rigidity K of the elastic support is variable depending on the applied reaction, an iterative calculation is required [15]:

$$K = \frac{\pi E_1}{2(1 - \gamma_1^2) \ln\left(\frac{0,2\pi a}{R\left(\frac{1 - \gamma_1^2}{E_1} + \frac{1 - \gamma_2^2}{E_2}\right)}\right)} \quad (1)$$

with $\gamma_1=0.16, \gamma_2=0.2, E_1=70000\text{MPa}$ and $E_2=200\ 000\text{MPa}$ Poisson's ratios and Young's modulus respectively of the single optical fiber and the metallic ribbon. $a=0.0625\text{mm}$, fiber radius.

So, for a given stiffness K , the resolution model is to adjust the external load applied to the massive so that the reaction tends to the solution R_0 (R_0 related to the stiffness by equation (1)).

The different steps of calculation are performed using the method of finite element discretization programmed into the CESAR-LCPC [16]. It's a software developed by the Laboratoire Central des Ponts et Chaussées (LCPC) since 1983 to resolve problems of civil engineering and industrial engineering. Figures 4 and 5 present the results of this study.

These curves show the behavior of the sensor as a function of the ribbon geometry for elastic massive under load. It can be seen that the reaction of the fiber, synonym of the sensor sensitivity, increases proportionally with the load before reaching the critical load previously determined by a geometrical parameter for small thicknesses ($e = 0.08\text{mm}$), figure 4, and a physical parameter for the large thicknesses, figure 5. This sensitivity is directly related to the dimensional characteristics of the ribbon (stiffness).

This study focused on the mechanical aspect to evaluate the stress field in the fiber. The impact of this field on the optical properties must be studied to apprehend the opto-mechanical response of the whole device.

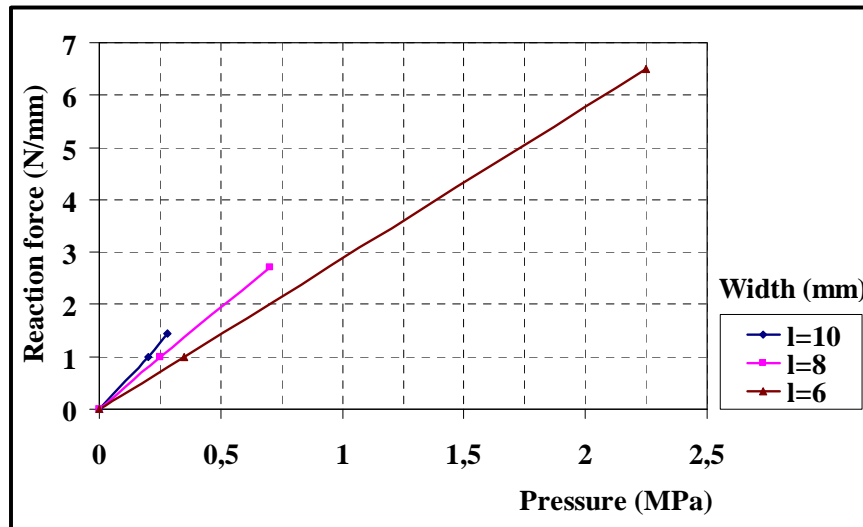


Figure 4: Sensor sensitivity as a function of applied pressure to the massive for e = 0.08mm

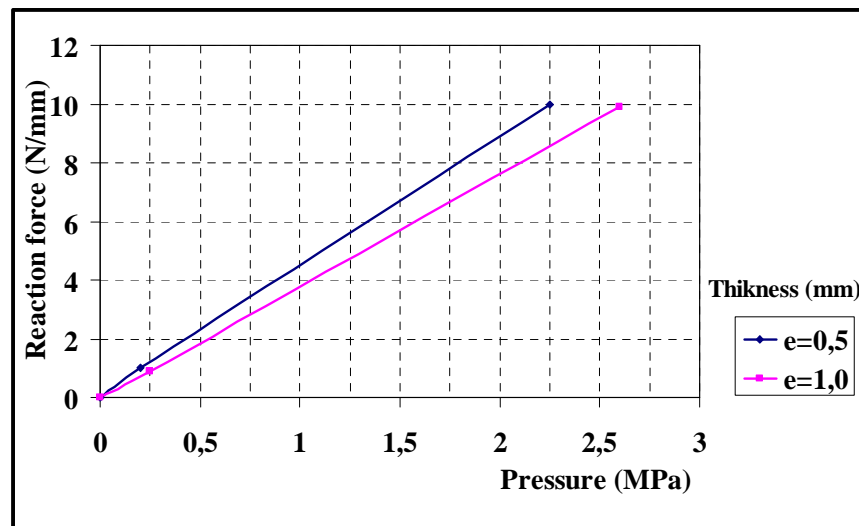


Figure 5: Sensor sensitivity as a function of applied pressure to the massive for l = 10mm

4. Coupled elasto-optical

The calculation of the reaction R , at the level of the optical fiber, produced by the ribbon under load depending on the number of polarimetric fringes m is given by [15]:

$$R = \frac{\pi d E \lambda}{4(1 + \gamma)(P_{12} - P_{11})n^3} m \quad (2)$$

where P_{11} and P_{12} are the characteristic components of the anisotropy of the silica. n , d , E , γ are respectively refractive index, diameter, Young's modulus and Poisson's ratio of the optical fiber and λ the wavelength of the laser source.

For a single mode fiber of the core diameter $d = 10 * 10^{-6} m$, illuminated by a light source of wavelength $\lambda = 1,3 * 10^{-6} m$ and following opto-mechanical characteristics : $n = 1,456$, $P_{11} = 0.121$, $P_{12} = 0.27$, $E = 7 * 10^{10} N/m^2$, $d = 10 * 10^{-6} m$ and $\gamma = 0,16$, the reaction of the fiber calculated from the equation (2) is equal to: $R = 16,74m$ (3)

Thus, the appearance of a polarimetric fringe corresponds to a reaction of ribbon equal to $16,74N$.

The number of fringes as a function of the pressure applied to the massive can be calculated using, on one hand the variation curves shown in figures 4 and 5 and, on other hand, the expression of equation (3).

So, $m = \frac{RL}{16,74}$, where L is the sensor length.

As an application, useful for the experimental study, we calculate the number of fringes as a function of the applied pressure, for ribbon thickness $e = 0,08mm$, width $l = 10mm$ and a length of interaction $L = 200mm$. The results are illustrated in figure 6.

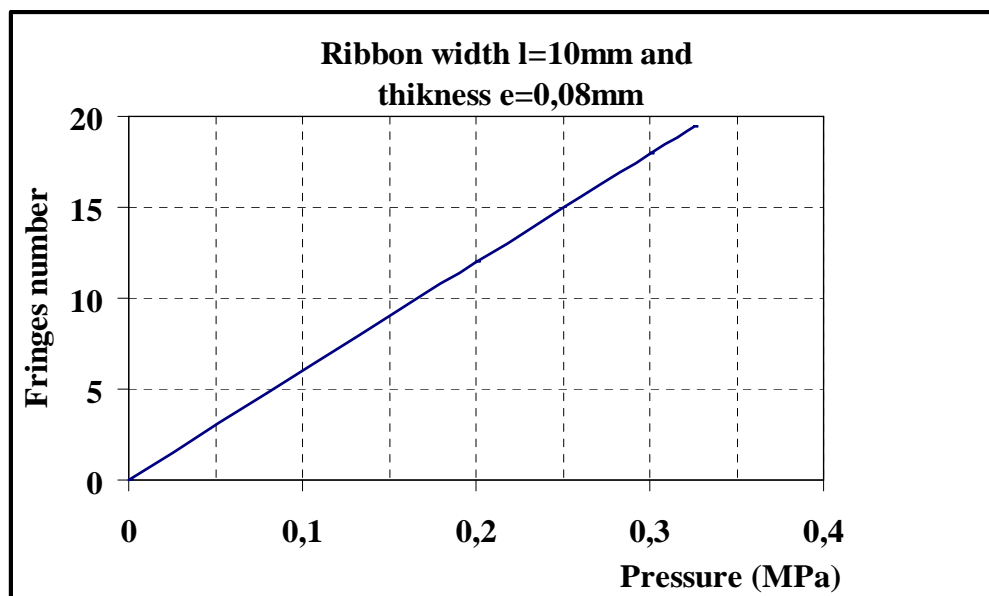


Figure 6: Sensor response versus applied load to massive for length of interaction $L = 200mm$

This curve shows the behavior of the number of fringes as a function of the applied load for elastic massive. The theoretical models should be corroborated by a series of experience to be sure of the practical feasibility to achieve such devices.

Conclusion and prospects

In this paper, we have sought to model the response of the sensor in its environment by studying numerically the global behavior involving both the sensor element but also the properties of the coating material. The deduced transfer function of the sensor is represented by reference graphs showing the sensitivity and the range. These two characteristics vary inversely, where improving one leads to restricting the other. The graphs constitute a practical way of sensor design adaptable to the user's needs.

Validation of models should be performed using laboratory model experiments. The results obtained can confirmed or not the feasibility of such device. However, to develop a complete system taking into account the sensitive element, its on-site calibration, head optoelectronics, acquisition, processing and exploitation of signals, we should have necessarily need an exploitation model related to the proprieties of the use envisaged.

Acknowledgements

The authors would like to express their sincere appreciation to IFSTTAR institute and to Alcatel Group for their encouragement, collaboration and support to perform this work.

References

1. Ungar S., *Fibres optiques : théorie et applications*, Edition Dunod. (1989).
2. Asawa C.K., Yao S. K., *Electronics letters*. 18 (1982) 362.
3. Bruinsma A.J.A., Van Zuylen P., *OFS* (1984) 399.
4. Abe T., Mistsunga Y., Koga H., *Optics letters*. 9 (1984) 373.
5. Khat A., Lamarque F., Puelle C., Pouille Ph., Leester-Schadel M., Buttgenbach S., *Sensors and Actuators A: Physical*. 158 (2010) 43.
6. Udd, E., Fiber optic sensor overview. In *Fiber Optic Smart Structures; Udd, E., Ed.*; Wiley: New York, NY, (1995); pp. 155-171.
7. Farhad Ansari, *Sensing issues in civil structural health monitoring*, Springer. (2005).
8. Glisic B. and Inaudi D., *Fibre optic methods for structural health monitoring*, JW & Sons, Ltd. (2007).
9. HVPParis'2008, (ICWIM 5 et HVTT 10), *Conférence Internationale sur les poids lourds, Paris*. (2008).
10. Kesavan K., Ravisankar K., Parivallal S., Sreeshylam P., Sridhar S., *Measurement*. 43 (2010) 157
11. Liang Tsair-Chun, Lin Yung-Li, *Optics Communications*. 285 (2012) 2363
12. Villalba S., Casas Joan R., *Mechanical Systems and Signal Processing*. (2012)
13. Teral S., Boby J., Siffert M., *Electrical Communication*. 1 (1994) 74
14. French Patent n° 88 02 765. (1988)
15. Barbachi M., Bourquin F., *MISC'11*. (2011) 201
16. Code CESAR-LCPC. *Manuel d'utilisation LCPC, Paris, France*. (2012).

(2012) ; <http://www.jmaterenvironsci.com>